Design of Double-Cladding Heterogeneous 2LP-Mode 6-Core Fiber with Two-Ring Layout

Zheyu Zhao
Grad. Sch. of Info. Sci. and Tech., Hokkaido University
Sapporo, Japan
zhao@icp.ist.hokudai.ac.jp

Takanori Sato
Grad. Sch. of Info. Sci. and Tech., Hokkaido University
Sapporo, Japan

Takeshi Fujisawa
Grad. Sch. of Info. Sci. and Tech., Hokkaido University
Sapporo, Japan

Taro Iawaya
Access Network Service Systems Labs NTT Corporation
Tsukuba, Japan

Yuto Sagae
Access Network Service Systems Labs NTT Corporation
Tsukuba, Japan

Taiji Sakamoto
Access Network Service Systems Labs NTT Corporation
Tsukuba, Japan

Takashi Matsui
Access Network Service Systems Labs NTT Corporation
Tsukuba, Japan

Kazuhide Nakajima
Access Network Service Systems Labs NTT Corporation
Tsukuba, Japan

Kunimasa Saitoh
Grad. Sch. of Info. Sci. and Tech., Hokkaido University
Sapporo, Japan

***Abstract*—Double-cladding heterogeneous 2LP-mode 6-core fibers (2LP-6CFs) with a two-ring layout are investigated. By optimizing core parameters in 125-µm cladding diameter, crosstalk in 2LP-6CF can be suppressed compared with that in heterogeneous 2LP-6CFs without double-cladding layer.**

Keywords*— *Double-cladding fibers, Heterogeneous multicore fibers, Few-mode fibers

I. INTRODUCTION

A few-mode multi-core fiber (FM-MCF) is beneficial for maximizing a spatial channel density [1] and achieving a large transmission capacity of over 10 Pb/s/fiber [2]. Although FM-MCFs with spatial channel count (SCC) exceeding 100, which is defined by the multiplication of the numbers of spatial channels, have been reported [3,4], their cladding diameters (CDs) are larger than 300 µm. Since a larger CD severely degrades the mass productivity, single-mode MCFs with a standard CD have been actively reported in recent years [5-7], and FM-MCFs with a 125-µm CD would also be preferable for practical applications. There are, however, technical limitations in designing FM-MCF with a 125-µm CD since a larger core pitch and cladding thickness are required to reduce the crosstalk (XT) and confinement losses of higher-order modes. So we have proposed an MCF with a double-cladding structure as a solution to these problems of the single cladding fiber [8].

In Ref. [8], an uncoupled-type 2LP-mode homogeneous 4-core fiber with the double-cladding layer has been reported, which achieved a relative core multiplicity factor (RCMF) of more than 10 for the first time among MCFs with a 125-µm CD while keeping the feasible XT and an effective area (A_{eff}). However, it is difficult to expand the number of cores with enough low XT. To further reduce the XT, the use of heterogeneous cores is effective. In addition, by using our previously proposed two-ring layout for single-mode heterogeneous MCFs (Hetero-MCFs) [9], it is expected that the number of cores in 2LP-mode MCF with a 125-µm CD can be increased with keeping low XT.

In this study, we propose a double-cladding heterogeneous 2LP-mode 6-core fiber (Hetero-2LP-6CF) with 125-µm CD for C-band use, which has the two-ring core layout. They are numerically investigated, and compared with the Hetero-2LP-6CF without a double-cladding profile. We confirmed that a designed double-cladding Hetero-2LP-6CF achieved an XT of LP_{11}-mode below −96 dB at 1 km for a wavelength of 1550 nm and A_{eff} = 80 µm^2. Furthermore, compared with the homogeneous double-cladding 4CF in [8], the SCC improves from 12 to 18 by using the two-ring core layout, keeping a lower XT value.

II. DESIGN OF 2-RING CORE LAYOUT WITH OUTER CLADDING

Fig. 1 illustrates a cross-sectional schematic of double-cladding Hetero-2LP-6CF and corresponding core refractive index profile which we considered in this paper, where n_1, n_2, and n_3 are the refractive indices in core, cladding, and outer cladding, respectively. Each core supports to propagate 2LP modes. The CD is set to be 125 µm.

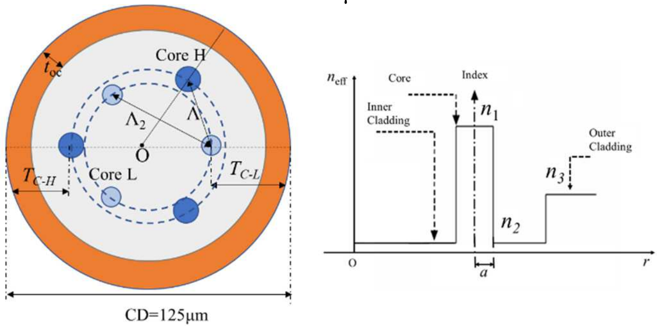

(a) (b)

Fig. 1 (a) Cross-section schematic of double-cladding Hetero-2LP-6CF with two-ring layout and (b) its refractive index profile.

As shown in Fig. 1(a), t_{oc} is outer cladding thickness. When $t_{\mathrm{oc}} = 0$, the structure becomes our previously proposed MCF with two-ring layout, except for the number of modes [9], in which two types of cores called core H (larger filled circle) and core L (smaller filled circle) are arranged alternately. The larger core radius tends to have low confinement loss to outer coating material, which means that core H can be placed outside rather than core L. In other words, to improve both the XT and confinement loss, the cladding thickness for core H ($T_{C\text{-}H}$) with a higher effective index (n_{eff}) can be smaller than that for core L ($T_{C\text{-}L}$) with a lower n_{eff}. To define the two-ring layout, we introduce the core pitch for core L as Λ_2, and the core pitch Λ indicates the distance between neighboring cores H and L. As described in [9], before determining the parameters of $T_{C\text{-}H}$ and $T_{C\text{-}L}$ for a two-ring layout, T_C (= $T_{C\text{-}H}$ = $T_{C\text{-}L}$) for a one-ring layout must be investigated. After that, the value of $T_{C\text{-}L}$ ($\geq T_{C\text{-}H}$) is searched for a two-ring layout, fixing the value of $T_{C\text{-}H}$ at T_C. Fig. 1(b) shows the refractive index profile of the core in the double-cladding Hetero-2LP-6CF, where point O refers to the center of the fiber, n_1, n_2, n_3 are the refractive indices of the core, inner cladding and outer cladding, respectively. Similar to [9], n_2 is set to 1.45 as a refractive index of pure silica, and when $r > 62.5$ μm (outside the fiber cladding), the refractive index is set to 1.486 as a coating material.

We start with T_C of 29 μm and increase it by 1 μm to select non-identical cores for Hetero-MCFs design. For the guided-mode analysis of a fiber, the finite element method (FEM) by the commercial software program (COMSOL) is used. Fig. 2 shows the distribution of bending loss (BL) at different core parameters, where a refers to the radius of the core and $\Delta = (n_1^2 - n_2^2)/2n_1^2$ is the relative refractive index difference between the core and the cladding. To guarantee 2LP-mode operation, the LP_{21} mode is required to be cutoff. Thus, the BL of LP_{21} mode should be larger than 1 dB/m at the wavelength of λ = 1530 nm and the bending radius of R_b = 140 mm, which is represented by the colored dashed lines in Fig. 2, whereas the excess loss (EL) of LP_{11} mode is required to be less than 0.01 dB/km at λ = 1565 nm and R_b = 140 mm, which is represented by the colored solid lines in Fig. 2. The solid black line denotes the contour line for A_{eff} = 80 μm^2 of LP_{01} mode at λ = 1550 nm. For the sake of homogeneity of transmission properties, the A_{eff} of non-identical cores are preferable to be equalized [10]. Therefore, core parameters that are on the black solid line (A_{eff} = 80 μm^2), and also surrounded by colored dashed and solid lines of the same color should be selected for the fiber design, referred to as the effective core region (ECR) like the red area between points M (lower BL limit) and N (upper cutoff limit) in Fig. 2 for C-band use. For a Hetero-MCF, neighboring core parameters can be determined from the lower limit and the upper limit of the ECR for each T_C value. For example, for T_C=33 μm they correspond to points M and N, respectively, as shown in Fig. 2. From Fig. 2, A_{eff}, EL, and cutoff lines intersect at the black point (A) when T_C = 29 μm. When T_C is less than 29 μm, the ECR will disappear, and thus T_C has to be equal or larger than 29 μm.

Compared with the MCF for t_{oc} = 0, a double-cladding fiber has an additional outer cladding layer ($t_{oc} > 0$ and $n_3 \neq n_2$). Although T_C = 29 μm is the minimum value for the MCF for t_{oc} = 0, we anticipate that the minimum value of T_C will be further reduced by properly adding the outer cladding layer. To evaluate a width of ECR, we define the effective refractive index (n_{eff}) difference of LP_{11}-mode between the upper cutoff limit (n_{eff} at the cutoff) and the lower BL limit (n_{eff} at the BL) of ECR as Δn_{ECR}. Fig. 3 shows Δn_{ECR} as a function of T_C, where Δ_2 (= $(n_3^2 - n_2^2)/2n_3^2$) is fixed to 0.3% and t_{oc} = 0, 8, 14, and 18 μm. Accordingly, $\Delta n_{ECR} < 0$ means that there is not a possible candidate of core parameter (a and Δ), so we have to ensure that $\Delta n_{ECR} > 0$ for each T_C value. As seen from the black line (t_{oc} = 0) in Fig. 3, $\Delta n_{ECR} > 0$ when $T_C \geq 29$ μm. Whereas, when t_{oc} = 14 μm, Δn_{ECR} becomes a positive value for $T_C \geq 27$ μm, which means that T_C can be reduced by setting Δ_2 = 0.3% and t_{oc} = 14 μm. However, when t_{oc} = 8 μm and 18 μm, such minimum T_C values become 33.7 and 27.5 μm. Therefore, we can find that the vicinity of t_{oc} = 14 μm seems to be an appropriate value.

In Fig. 3, fluctuations of Δn_{ECR} can be seen in values of $t_{oc} >$ 0. Note that the Δ of the core has to be decreased as the T_C increases. When the distance between the core and the outer cladding increases with T_C, the coupling of the core mode to the outer cladding mode becomes weak, resulting in a decrease of BL of the LP_{21}-mode group. In order to meet the cutoff condition of the LP_{21} mode (BL>1dB/m), the core parameters (a and Δ) need to be changed significantly, which eventually resulting in a decrease of Δn_{ECR}.

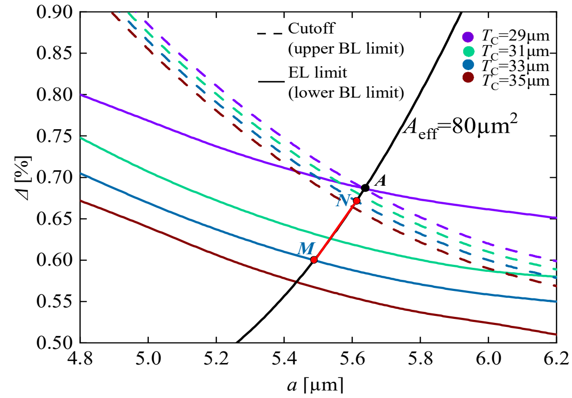

Fig. 2. The core parameters (core radius a and core Δ) and its relationship of cutoff region, EL limit, and A_{eff} at λ =1550 nm, where t_{oc} = 0 and T_C = 29, 31, 33, and 35 μm.

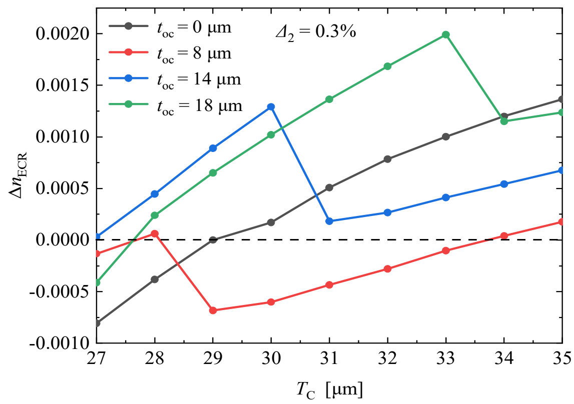

Fig. 3. Δn_{eff} for LP_{11} modes between neighboring cores in double-cladding Hetero-2LP-6CF as a function of T_C, where Δ_2 = 0.3% and t_{oc} = 0 (without a double-cladding layer), 8, 14, and 18 μm.

III. Crosstalk Evaluation

As described in the previous section, we set t_{oc} = 14 μm and Δ_2 = 0.3% from here. As same as Fig. 2, we can plot the core parameter map as shown in Fig. 4. It is known that the XT of Hetero-MCF considerably decreases when the bending radius (R_b) becomes larger than the critical value of the bending radius (R_{pk}), which is defined as

$$R_{\mathrm{pk}} = \frac{n_{\mathrm{eff}}}{\Delta n_{\mathrm{eff}}}\Lambda, \qquad (1)$$

where n_{eff} is the effective refractive index of the core, and the Δn_{eff} is the refractive index difference between the cores of

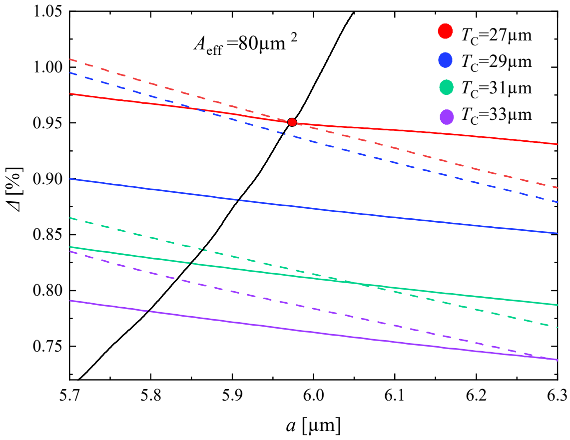

Fig. 4. The core parameters (core radius a and core Δ) and its relationship of cutoff region, EL limit, and A_{eff} at λ =1550 nm, where t_{oc} = 14 μm, Δ_2 = 0.3%, and T_{C} = 27, 29, 31, and 33 μm.

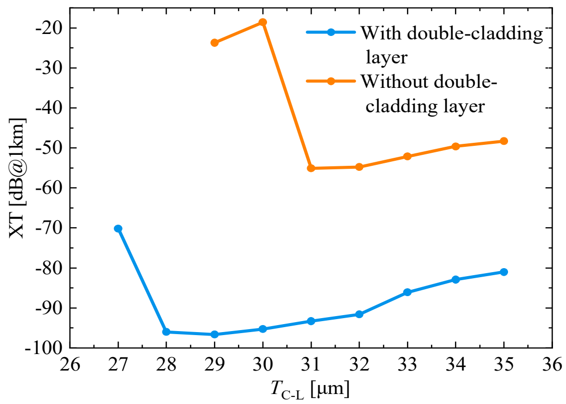

Fig. 5. Comparison of XT between the Hetero-2LP-6CFs with the double-cladding layer ($T_{\mathrm{C\text{-}H}}$ = 27 μm, t_{oc} = 14 μm and Δ_2 = 0.3%) and without double-cladding layer ($T_{\mathrm{C\text{-}H}}$ = 29 μm, t_{oc} = 0 μm), where λ = 1550 nm.

Hetero-MCFs. The XT converges on a certain value for enough larger R_{b} [11,12]. Accordingly, we should set

$$\Delta n_{\mathrm{eff}} > \frac{n_{\mathrm{eff}}}{R_{\mathrm{b}}}\Lambda. \qquad (2)$$

When T_{C} increases, Δn_{eff} increases since the width between the upper and lower limits in Fig. 2 increases. On the contrary, Λ decreases for a larger T_{C}, resulting in the degradation of XT. The main objective for designing Hetero-MCFs is to find non-identical adjacent core parameters with a large enough Δn_{eff} and Λ. If different cladding thicknesses ($T_{\mathrm{C\text{-}H,\,C\text{-}L}}$ in Fig. 1(a)) of two-ring layout Hetero-MCFs are chosen, we can make Δn_{eff} for LP_{11} modes between non-identical cores larger while suppressing the decrease of Λ. To maximize the suppression of the XT, it is better to fix $T_{\mathrm{C\text{-}H}}$ = 27 μm for high-index core and search $T_{\mathrm{C\text{-}L}}$ for low-index core in a range of $T_{\mathrm{C\text{-}L}}$ > 27 μm. Fig. 5 shows the comparison of XT between the Hetero-2LP-6CFs without double-cladding layer (t_{oc} = 0 μm) and with double-cladding layer (t_{oc} = 14 μm and Δ_2 = 0.3%), where λ = 1550 nm and $T_{\mathrm{C\text{-}H}}$ = 27 μm. To calculate the XT, we take the same procedure in [9], and we set the correlation length d = 1 m, and the bending radius R_{b} = 140 mm. For all $T_{\mathrm{C\text{-}L}}$, XTs of the double-cladding Hetero-2LP-6CF are improved compared with those of without double-cladding layer. The smallest XT of −96 dB@1km can be obtained when $T_{\mathrm{C\text{-}H}}$ = 27 μm, $T_{\mathrm{C\text{-}L}}$ = 29 μm, t_{oc} = 14 μm, and Δ_2 = 0.3%. This XT value is lower than that in the homogeneous 2LP-4CF, which is −55 dB@1km. These results show that the proposed heterogeneous FM-MCF with outer cladding layer structure is beneficial for achieving the effective use of core and mode multiplexing in a limited CD.

IV. Conclusion

The double-cladding Hetero-2LP-6CF with a two-ring layout is investigated, in which CD is 125 μm. The XT of less than −96 dB@1km can be achieved by using an outer cladding layer structure. It is lower than the XTs in the homogeneous 2LP-4CF and Hetero-2LP-6CF without double-cladding layer. It proves that double-cladding Hetero-2LP-6CF with a two-ring layout is beneficial for reducing inter-core crosstalk and achieving a 125-μm CD MCF with higher spatial multiplicity.

References

[1] T. Sakamoto, K. Saitoh, S. Saitoh, Y. Abe, K. Takenaga, A. Urushibara, M. Wada, T. Matsui, K. Aikawa, and K. Nakajima, "Spatial density and splicing characteristic optimized few-mode MCF," J. Lightw. Technol., vol. 38, no. 16, pp. 4490-4496, Apr. 2020.

[2] D. Soma, Y. Wakayama, S. Beppu, S. Sumita, T. Tsuritani, T. Hayashi, T. Nagashima, M. Suzuki, M. Yoshida, K. Kasai, M. Nakazawa, H. Takahashi, K. Igarashi, I. Morita, and M. Suzuki, "10.16 peta-b/s dense SDM/WDM transmission over 6-mode 19-core fiber across the C+L band," J. Lightw. Technol., vol. 36, no. 6, pp. 1362-1368, Jan. 2018.

[3] J. Sakaguchi, W. Klaus,J.-M.D. Mendinueta,B.J. Puttnam,R.S. Luis,Y. Awaji,N. Wada,T. Hayashi,T. Nakanishi,T. Watanabe,Y. Kokubun, T. Takahata, and T. Kobayashi., "Realizing a 36-core, 3-mode fiber with 108 spatial channels," Proc. Opt. Fiber Commun. Conf. (OFC), Paper Th5C.2, Mar. 2015.

[4] K. Igarashi, D. Souma,Y. Wakayama, K. Takeshima, Y. Kawaguchi, T. Tsuritani, I. Morita, and M. Suzuki., "114 space-division-multiplexed transmission over 9.8-km weakly-coupled-6-mode uncoupled-19-core fibers," Proc. Opt. Fiber Commun. Conf. (OFC), Paper Th5C.4, Mar. 2015.

[5] T. Matsui, T. Sakamoto, Y. Goto, K. Saito, K. Nakajima, F. Yamamoto, and T. Kurashima, "Design of 125 μm cladding multi-core with full-band compatibility to conventional single-mode fiber," Proc. Eur. Conf. Opt. Commun. (ECOC), Paper We.1.4.5, Sept. 2015.

[6] T. Gonda, K. Imamura, M. Tsukamoto, K. Kawasaki, S. Arai, R. Sugizaki, S. Beppu, D. Soma, H. Takahashi, T. Tsuritani, "Design of MCF having upgradability from standard single-mode fibers and its application," J. Lightw. Technol., vol. 37. No. 2, pp. 396-403, Jan. 2019.

[7] Y. Sagae, T. Matsui, T. Sakamoto, and K. Nakajima, "Ultra-low crosstalk MCF with standard 125- μm CD for 10,000 km-class long-haul transmission," IEICE Transactions on Communications, vol. E103-B, no. 11, pp. 1199-1205, Nov. 2020.

[8] Y. Sagae, T. Matsui, T. Sakamoto, T. Iwaya, T. Mori, T. Sato, K. Saitoh, K. Nakajima, "A 125-μm CD uncoupled 3-mode 4-core fibre with the highest core multiplicity factor," 2022 ECOC, Basel, Switzerland, paper Tu3A.2. , Sept. 2022.

[9] Y. Wang, T. Fujisawa, Y. Sagae, T. Sakamoto, T. Matsui, K. Nakajima, K. Saitoh, "A novel core allocation in heterogeneous step-index MCFs with standard CD," J. Lightw. Technol., vol. 39, no. 22, pp. 7231-7237, Nov. 2021.

[10] S. Matsuo, K. Takenaga, K. Saitoh, K. Nakajima, Y. Miyamoto, T. Morioka, "High-spatial-multiplicity MCFs for future dense space-division-multiplexing systems," J. Lightw. Technol., vol. 34, no. 6, pp. 1464–1475, Mar. 2016.

[11] T. Hayashi, T. Taru, O. Shimakawa, T. Sasaki, and E. Sasaoka, "Design and fabrication of ultra-low crosstalk and low-loss MCF," Opt. Exp., vol. 19, no. 17, pp. 16576-16592, Aug. 2011.

[12] T. Fujisawa, Y. Amma, Y. Sasaki, S. Matsuo, K. Aikawa, K. Saitoh, and M. Koshiba, "Crosstalk analysis of heterogeneous multicore fibers using coupled-mode theory," IEEE Photonics Journal, vol. 9, no. 5, pp. 1-8, Oct. 2017